ChemPubSoc Europe

DOI: 10.1002/cbic.201600092

CHEMBIOCHEM Communications

SPECIAL ISSUE

The Effects of Spacer Length and Composition on Aptamer-Mediated Cell-Specific Targeting with Nanoscale PEGylated Liposomal Doxorubicin

Hang Xing[+],[a] Ji Li[+],[a] Weidong Xu,[c] Kevin Hwang,[a] Peiwen Wu,[a] Qian Yin,[b] Zhensheng Li,[a] Jianjun Cheng,[b] and Yi Lu*[a]

Aptamer-based targeted drug delivery systems have shown significant promise for clinical applications. Although much progress has been made in this area, it remains unclear how PEG coating would affect the selective binding of DNA aptamers and thus influence the overall targeting efficiency. To answer this question, we herein report a systematic investigation of the interactions between PEG and DNA aptamers on the surface of liposomes by using a series of nanoscale liposomal doxorubicin formulations with different DNA aptamer and PEG modifications. We investigated how the spatial size and composition of the spacer molecules affected the targeting ability of the liposome delivery system. We showed that a spacer of appropriate length was critical to overcome the shielding from surrounding PEG molecules in order to achieve the best targeting effect, regardless of the spacer composition. Our findings provide important guidelines for the design of aptamer-based targeted drug delivery systems.

Pharmaceutical drug delivery systems on the nanometer scale have been widely used as nanocarriers to boost drug efficacy. When compared with their free drug counterparts, drugs encapsulated in nanocarriers can display higher stability, fewer side effects, and more controllable release kinetics. In order to maximize their therapeutic potential, a tremendous amount of effort has been devoted toward studying how the physical properties of nanocarriers, such as size, shape, rigidity, charge, and surface function, can influence their interactions with targeted cells and thus the efficiency of delivery to the relevant tissues.[1] Among many physical properties, the surface properties of nanocarriers play a central role, as the interface between the delivery vehicle and the biological components in and on cells during the delivery process determines the stability, targeting ability, and kinetics of drug release of the nanocarriers.[1f,2] Therefore, nanocarrier surfaces have been functionalized with active biorecognition agents that can bind to specific receptors on the cell surface, allowing selective accumulation of nanomedicine into diseased tissues but not normal tissues.[3]

Among the types of biorecognition agents utilized to enhance selectivity of nanocarriers, DNA aptamers, which are single-stranded oligonucleotides that can selectively bind to target molecules, have emerged as a promising class of targeting ligand due to their higher stability and lower cost than antibodies, another common class of biorecognition agent for targeted therapy. Moreover, aptamers against different targets of interest can be selected through the systematic evolution of ligands by exponential amplification (SELEX) process, providing the possibility of developing nanomedicines for specific cells and tissues.[4] These features, together with non-immunogenicity and ease of preparation and functionalization onto nanocarriers, make aptamers an excellent choice as a class of biorecognition agents for nanomedicine.[5] Indeed, many DNA aptamer-functionalized nanocarriers have been used for successful delivery of drugs both in vitro and in vivo.[5a,6]

Despite the enhanced selectivity stemming from specific surface interactions between biorecognition molecules, such as aptamers, and the target receptors on the disease cells, the targeted delivery process is complicated by other biological components under physiological conditions.[7] A number of literature reports have demonstrated that serum proteins can absorb onto nanoparticle surfaces to form a protein corona.[8] Nonspecifically adsorbed serum proteins affect the physiological properties of nanocarriers and can mask their targeting capabilities toward cell receptors, thereby leading to a loss of recognition specificity and fast clearance by the reticuloendothelial system (RES).[9] To suppress nonspecific serum protein adsorption, antifouling polymers such as polyethylene glycol (PEG) have been used to backfill the surface of nanocarriers, allowing a much longer circulation time in blood and a higher chance of nanocarrier accumulation in the desired tissue.[10] Although the use of PEG modifications to inhibit protein adsorption has been widely reported, the interaction between backfilling PEG molecules and neighboring recognition molecules on the same surface has not been thoroughly studied.[5a,6c] A few studies have reported that the PEG shield on the nanopar-

[a] H. Xing,[+] J. Li,[+] K. Hwang, P. Wu, Z. Li, Prof. Y. Lu
Department of Chemistry, Beckman Institute for Advanced Science and Technology
University of Illinois at Urbana–Champaign
405 N Mathews Avenue, Urbana, IL 61801 (USA)
E-mail: yi-lu@illinois.edu

[b] Q. Yin, Prof. J. Cheng
Material Science and Engineering, Beckman Institute for Advanced Science and Technology
University of Illinois at Urbana–Champaign
405 N Mathews Avenue, Urbana, IL 61801 (USA)

[c] W. Xu
Department of Chemistry, Tsinghua University
Beijing 100084 (China)

[+] These authors contributed equally to this work.

Supporting information and the ORCID identification number(s) for the author(s) of this article can be found under http://dx.doi.org/10.1002/cbic.201600092.

This manuscript is part of a Special Issue on DNA Nanotechnology.

ticle surface can sterically hinder the binding of antibodies or peptides to a receptor target, and appropriate backfilling PEG length is critical to achieve optimal cellular uptake.[2a,11]

In order to design aptamer-based nanoscale drug delivery systems for effective clinical applications, it is important to carry out systematic studies of the interactions between the targeting aptamers and the backfilling PEG molecules in order to find the optimal parameters to maximize the targeting effect while minimizing non-specific interactions. To achieve this goal, we used a PEGylated liposomal doxorubicin (PEG-Lip-Dox) with a DNA aptamer attached to the surface of the liposome as the model system to investigate the effect of spacer length and PEG modification on aptamer-mediated cell-specific targeting. We choose liposomes for this investigation, because they are one of the most successful drug delivery systems due to inherent advantages such as high drug-loading efficiency and biocompatibility.[5a,6c,12] Furthermore, a PEG-Lip-Dox, Doxil, was the first nanomedicine formulation approved by the United States Food and Drug Administration (FDA) for treating a variety of cancers.[13,14] Therefore, the knowledge gained from this study can be readily translated into clinical applications.

In previous studies, we have demonstrated that a PEGylated liposome system containing anticancer drugs such as cisplatin or Dox can be effectively functionalized on its surface with a DNA aptamer called AS1411, which can selectively recognize nucleolin (NCL), an mRNA-stabilizing protein overexpressed on the plasma membrane of many types of cancer cells, including breast cancer cells.[5a,6c] We further showed that this targeted liposomal Dox construct was able to facilitate selective drug uptake into breast cancer cells[5a] and allowed enhanced tumor penetration and antitumor efficacy in MCF-7 tumor models in mice.[6c] Although these results are encouraging, it remains unclear how the PEG coating would affect the selective binding of the NCL target by the DNA aptamer and thus influence the overall targeting efficiency. To clarify this issue, we report herein a systematic investigation of the interactions between PEG and DNA aptamers by preparing a series of liposomal Dox formulations with different DNA aptamer and PEG modifications, as well as a determination of how the spatial size and composition of the spacer molecules on the surface of the liposome affect the targeting ability of the liposome delivery system toward breast cancer cells.

The formulation of the liposomal Dox with PEG and aptamer modifications was based on Doxil, an FDA-approved, Dox-containing liposome with no targeting ligand incorporated.[14] We modified this liposome with different aptamers to make it target-specific. The liposome was formulated from hydrogenated soy phosphatidylcholine (HSPC) and cholesterol (chole) at a molar ratio of 2:1.[15] The cholesterol was added into the system, as it increases the hydrophobic–hydrophobic interactions within the lipid bilayer and therefore improves the rigidity and stability of liposomes.[15] Distearoyl phosphatidyl-ethanolamine (DSPE)-modified methoxy-PEG with a molecular weight (MW) of 5000 Da or 2000 Da (mPEG5000 and mPEG2000, respectively) was applied as a protecting element to backfill the liposomal surface at a molar ratio of ~6% of

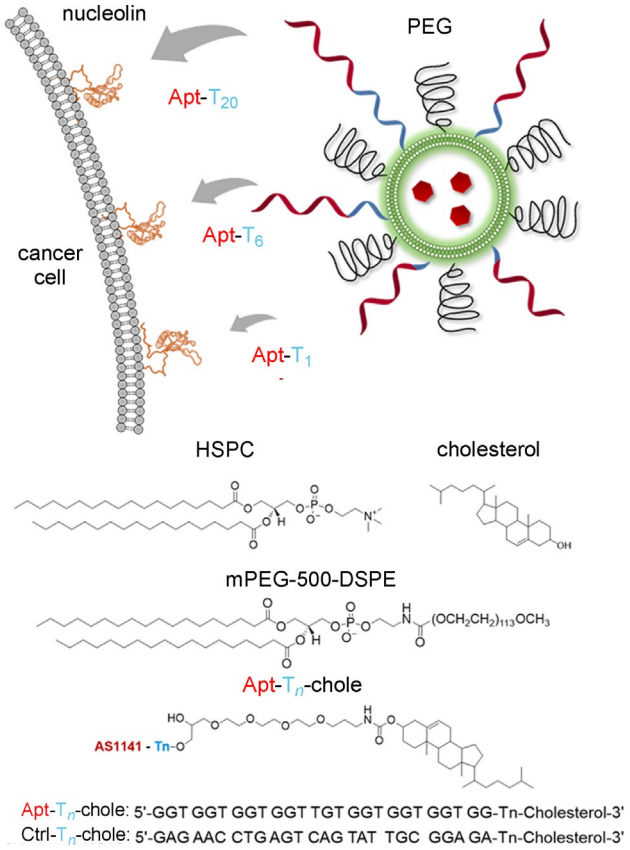

Figure 1. Schematic of the targeting ability of PEGylated liposomal doxorubicin (PEG-Lip-Dox), modified with DNA aptamer AS1411 by using oligo-T sequences of different lengths as spacers, towards breast cancer cells through specific binding of AS1411 to nucleolin on cell membranes. HSPC, cholesterol, and mPEG-DSPE (mPEG2000-DSPE or mPEG5000-DSPE) were combined in a 2:1:0.16 molar ratio. Cholesterol-modified DNA strands were immobilized onto the liposomal surface by intercalating the 3′ cholesterol modification into the lipid bilayer.

total lipid content (Figure 1). The combination of HSPC and cholesterol provides liposomes with a high phase transition temperature of 48 °C, as well as high rigidity and low permeability under physiological conditions.[15] Dox, an anticancer drug as well as a fluorescent probe, was encapsulated into the liposome through a pH–ion gradient loading method.[16] This well-established formulation of PEGylated liposomes has been used in clinical practice for cancer treatment for decades. To introduce the targeting ability of PEG-Lip-Dox, AS1411, a 26-mer NCL aptamer (Apt) with the sequence 5′-GGT GGT GGT GGT TGT GGT GGT GGT GG-3′ was used as a targeting agent for breast cancer cells, and a scrambled strand of the same length (Ctrl) with the sequence 5′-GAG AAC CTG AGT CAG TAT TGC GGA GA-3′ was applied as the non-targeting control agent. Both DNA strands were functionalized with cholesterol at the 3′-end, serving as an anchor to the lipid bilayer to immobilize the sequences to the surface of the liposome (Figure 1).

Previous studies of aptamers or DNAzymes on surfaces indicate that the presence of other molecules on the same surface can affect the target-binding ability of the aptamers or DNAzymes.[17] Based on these results, we hypothesized that the

PEG coating on the liposome surface could also sterically interfere with the binding ability of the DNA aptamer. To minimize this interference, the complete aptamer sequence should be fully exposed above the backfilling PEG molecules. To achieve this goal, we introduced a spacer between the cholesterol anchor to the liposome and the aptamer recognition sequence in order to expose the aptamer above the PEG layer. Therefore, the length of the spacer could have significant impact on the targeting ability of PEG-Lip-Dox and thus should be properly designed in order to overcome the interference of the surrounding backfilling PEG. To meet this criterion, we chose oligo-thymine (oligo-T) as the spacer and controlled the length of the spacer by using different numbers of thymine bases (Apt-T_n, where *n* represents the length of the oligo-T spacer; Figure 1).

To guide the design of the experiment, molecular dynamics (MD) simulations were conducted on PEG5000 and oligo-T spacers by using the Discover module in Material Studio 7.0 to estimate the length of each spacer at room temperature (298 K) and ambient atmospheric pressure (0.1 GPa) in water. As shown in Figure 2, the length of PEG5000 was estimated to be ~58 Å; the oligo-T spacers with lengths T_1, T_6, and T_{20} were ~17, ~32, and ~56 Å, respectively. Therefore, the AS1411 sequences with different lengths of spacers on the PEG-Lip-Dox surface represent three different levels of exposure to PEG on the liposome surface: mostly embedded (T_1), partially exposed (T_6), and mostly exposed (T_{20}).

To experimentally confirm the above MD simulation results, the AS1411 aptamer-modified PEG-Lip-Dox samples with the aptamer sequence linked to T_1, T_6, and T_{20}, with cholesterol at the 3′-end (Figure 1), were prepared by using 100 nm polycarbonate-membrane-supported extruders in 130 mM $(NH_4)_2SO_4$ buffer (pH 5.5) with 10% *w/v* sucrose, based on previously published protocols.[5a,6c] DNA loading on liposomes with ~6% PEG modification could be maximized to a DNA-to-lipid ratio of ~0.3 nmol mg^{-1}. After the liposome was formed, Dox was loaded into the liposome by using a pH–ion gradient loading method in 10 mM histidine buffer (pH 6.5) with 300 mM sucrose to reach a high loading efficiency. Size-exclusion chromatography was applied to remove free Dox. The resulting Apt-PEG-Lip-Dox sample was concentrated by centrifugation.

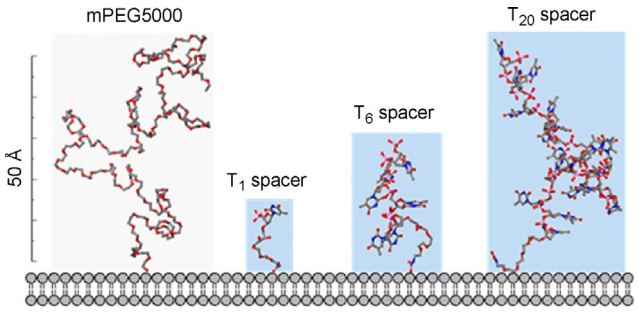

Figure 2. Molecular dynamics simulation of PEG5000 and three oligo-T spacers of T_1, T_6, and T_{20} by using the Discover module in Material Studio 7.0. The length of PEG5000 is estimated to be ~58 Å, with T_1 of ~17 Å, T_6 of ~32 Å, and T_{20} of ~56 Å.

To elucidate the morphology of the liposome sample, cryo-electron microscopy (cryo-EM) data were collected that showed the liposomal Dox samples exhibited a coffee-bean-like shape with rod-shaped Dox solids in the middle of the liposomes. The length of Apt-PEG-Lip-Dox was ~170 nm, with a width of ~120 nm, which is consistent with the morphology of commercial samples without the aptamer on the surface, suggesting successful and efficient loading (Figure 3A).[18] The Dox concentration in the Apt-PEG-Lip-Dox sample was quantified by UV/Vis absorption at 480 nm after treatment with a solution of 90% isopropanol and 10% 0.075 M HCl to fully rupture the liposome. By using a standard UV/Vis absorption curve for free Dox, the equivalent Dox concentration of a DNA-modified PEG-Lip-Dox sample could reach high Dox loading (~2 mg mL^{-1}) after tuning the concentration (Figure S1).

To evaluate the stability of the Apt-PEG-Lip-Dox formulation, fluorescence emission at 592 nm with excitation at 480 nm was monitored after incubation in 50% human serum at 37 °C over a period of 24 h. As shown in Figure 3B, only ~5% of the maximum possible enhancement of fluorescence intensity was observed after 10 h incubation, and less than 15% of maximum leakage could be detected after 24 h incubation, suggesting low levels of decomposition of the liposome samples and thus minimal leakage of encapsulated Dox. These results indicated that the Apt-PEG-Lip-Dox samples were highly stable in 50% human serum, with well-preserved fluorescent properties.

To systematically investigate the effect of the length of the oligo-T spacer on the steric interaction between targeting agent and backfilling PEG, PEG5000-protected liposomal Dox samples were prepared, functionalized with AS1411 aptamer or control DNA sequences and with T_1, T_6, and T_{20} as spacers. Dynamic light scattering (DLS) and zeta-potential measurements were carried out to investigate the effect of DNA modification on hydrodynamic radius and surface charge of the liposome sample in the Apt-PEG-Lip-Dox samples with different T_n spacers prior to loading Dox. PEG-Lip-Dox without DNA modification had a hydrodynamic size of 158 ± 15 nm and a surface zeta-potential of −3.4 ± 2.2 mV. After DNA functionalization, the Apt-PEG-Lip-Dox samples had a ~20 nm increase in diameter and a ~10 mV decrease in surface zeta-potential (Figure 3C), which was attributed to the modification of negatively-charged DNA strands on the surface.[19] Interestingly, varying the spacer lengths from T_1 to T_{20} had minimal effects on the physical properties of the liposome samples, as evidenced by the similar hydrodynamic radius and surface zeta-potentials for T_1, T_6, and T_{20} samples (Figure 3C).

The concentration of the lipids in each sample was measured at a fluorescence emission of 627 nm by using Nile Red-stained Apt-PEG-Lip samples without Dox loaded inside the liposome (Figure S2). The DNA density on each liposome sample was also measured by using SYBR Green II dye without Dox loaded inside the liposome (Figure S3). The results showed that the lipid and DNA concentrations were similar for each sample, even with different spacer lengths, and the DNA could reach a final concentration of ~2 μM (Figure S4).

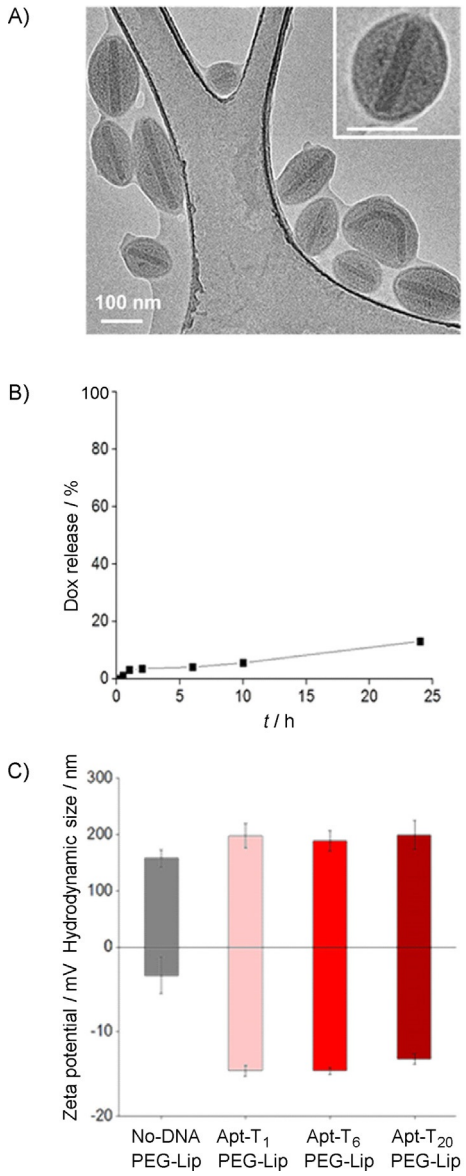

Figure 3. A) Cryo-EM micrographs of a DNA-modified PEG-Lip-Dox sample. The length of the liposomal Dox is ~170 nm, with a width of ~120 nm. B) Time course study of Dox release from liposomes at 37 °C in 50% human serum. C) Representative DLS and zeta-potential measurements of different liposome samples (No-DNA-PEG-Lip, Apt-T_1-PEG-Lip, Apt-T_6-PEG-Lip, and Apt-T_{20}-PEG-Lip). The reported hydrodynamic size and zeta-potential of liposome samples were calculated from the average of three measurements. Error bars represent the standard deviation.

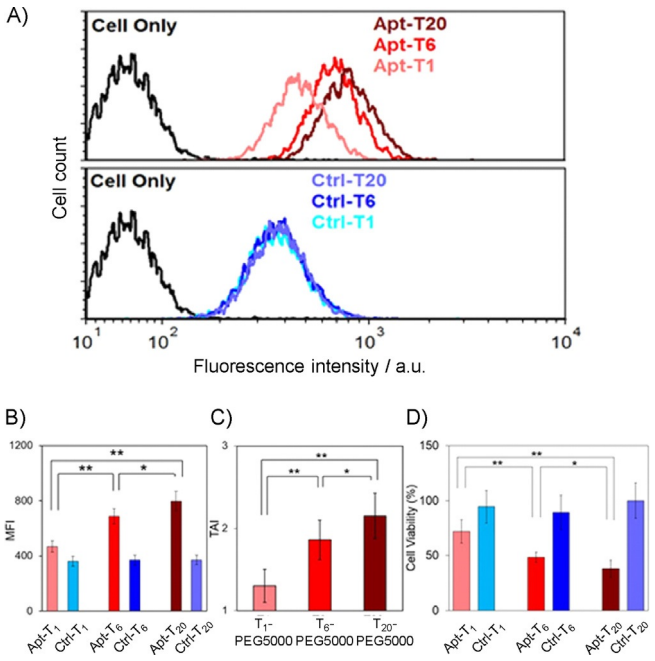

Figure 4. A) Flow cytometry analysis of MDA-MB-231 breast cancer cells treated with Apt- or Ctrl-linked T_1-Lip-Dox, T_6-Lip-Dox, and T_{20}-Lip-Dox samples. MDA-MB-231 cells (200000 per well) were plated in 12-well plates. The cells were treated with liposomal Dox samples (equivalent to 20 μM Dox) at 37 °C for 2 h. B) Geometric mean fluorescence intensity (MFI) of MDA-MB-231 cells treated with liposomal Dox. C) Targeting ability index (TAI) of liposomal Dox. TAI = MFI (Apt)/ MFI (Ctrl). D) Cytotoxicity study of Ctrl-Lip-Dox and Apt-Lip-Dox samples. MDA-MB-231 cells (3000 cells per well) were plated in a 96-well plate 24 h before study. MDA-MB-231 cells were treated with DNA-modified liposomal Dox samples at a concentration equivalent to 10 μM Dox at 37 °C for 6 h. The cells were then washed and incubated in media for a total of 72 h before assessing cell viability by MTT assay in each group. Error bars represent the standard deviation of three experiments. $*p < 0.05$, $**p < 0.01$, Student's *t*-test.

To investigate the targeting capability of Apt-PEG-Lip-Dox, the Dox-loaded liposomes functionalized with the AS1411 aptamer linked to different oligo-T spacers (Apt-T_n-PEG-Lip-Dox) or the control DNA linked to different oligo-T spacers (Ctrl-T_n-PEG-Lip-Dox), diluted to the same equivalent Dox concentrations (20 μM), were incubated with MDA-MB-231 human breast cancer cells for 2 h. The treated cells were then washed, trypsinized, and fixed in 4% paraformaldehyde solution for flow cytometry analysis to measure fluorescence intensity. As shown in Figure 4A, the geometric mean fluorescence intensity (MFI) in cells treated with Apt-T_n-PEG-Lip-Dox was significantly higher than that of cells treated with corresponding Ctrl-T_n-PEG-Lip-Dox (Figure 4A), indicating the targeting effect of the AS1411 sequence to MDA-MB-231 cells. When comparing the MFI of all Apt-T_n samples with different spacer lengths, Apt-T_{20} exhibited higher MFI in treated cells than did Apt-T_6 ($*p < 0.05$), with Apt-T_1 exhibiting a significantly lower MFI in comparison to T_{20} and T_6 samples ($**p < 0.01$; Figure 4B). According to the estimated lengths of PEG5000, T_1, T_6, and T_{20} from MD simulations, the degree of AS1411 exposure in a PEG-backfilled surface increased as the length of the oligo-T sequence increased. Therefore, the observation of enhanced targeting capability with the increase in length from T_1 to T_6 to T_{20} can be attributed to the increased exposure of the aptamer sequence on the surface of liposomes, suggesting that the biorecognition ability of the aptamer could be affected by steric hindrance from the protective PEG layer.[20] Although most aptamer sequences were expected to be embedded in the PEG backfill layer with the T_1 linker, a small portion of aptamers might still be exposed from the PEG and remain functional, due to the dynamic structure of the lipid bilayer and possible non-uniform DNA distribution, resulting in slightly higher binding affinity for Apt-T_1 samples than Ctrl-T_1 samples.

In order to obtain a quantitative estimation of the targeting ability of Apt-PEG-Lip-Dox samples, we defined the targeting ability index (TAI), which was calculated as follows:

$$TAI = MFI(Apt)/MFI(Ctrl)$$

Theoretically, the TAI for non-targeting samples is 1 when the sample MFI is equal to the control MFI. A higher TAI indicates improved targeting effects of the Apt-T_n-PEG-Lip-Dox sample to MDA-MB-231 cells. Figure 4C shows that the average TAI increased from 1.30 to 1.86 to 2.15 as the linker increased from T_1 to T_6 to T_{20}, suggesting increased targeting ability for longer spacers. Moreover, the targeting ability for the T_6 linker was closer to that of T_{20} linker rather than to the T_1 linker, which could be attributed to the protein binding to the exposed GGT units of the aptamer sequence and the flexibility of the surrounding PEG molecules.

To corroborate the effect of spacer length on the cellular uptake of Apt-PEG-Lip-Dox samples, we investigated the cytotoxicity of Apt-PEG-Lip-Dox samples with different T_n spacers. In order to give the MDA-MB-231 cells enough time for uptake of Apt-PEG-Lip-Dox samples in the cytotoxicity test, cells were incubated with Apt-T_n-PEG-Lip-Dox or Ctrl-T_n-PEG-Lip-Dox samples with the same Dox concentration (10 μM) for 6 h, followed by 24 h of cell growth before measuring cell viability by using the MTT assay. As shown in Figure 4D, all Apt-T_n-PEG-Lip-Dox samples exhibited significantly higher cytotoxicity than the corresponding Ctrl-T_n-PEG-Lip-Dox samples (**$p < 0.01$), confirming the targeting ability of the aptamer over the control DNA. More interestingly, cell viabilities were 71 ± 6, 48 ± 5, and 38 ± 8% for cells treated with Apt-T_n-PEG-Lip-Dox samples with T_1, T_6, and T_{20} spacers at the same Dox concentrations, indicating decreased cell viability with increasing in T_n spacer length. As the cell viability depends mainly on the amount of Dox delivered into the cells, the highest antiproliferative activity of the Apt-T_{20}-modified Lip-Dox construct indicates that this construct was best internalized by the MDA-MB-231 cells. In comparison, the Apt-T_1 sample was internalized the least by MDA-MB-231 cells, indicating the lowest binding affinity to surface NCL biomarkers, further confirming the steric hindrance of the PEG backfill, due to the difference in spacer length.

After demonstrating that the length of the oligo-T spacer was critical to the targeting ability of the AS1411 aptamer, it was also important to investigate whether a different type of spacer with a similar length but different composition would affect the targeting ability. To achieve this goal, we designed a spacer consisting of oligo-T linked to PEG2000 and compared it with the T_{20} spacer. First, MD simulations were used to find out the length of oligo-T needed to conjugate to PEG2000 in order to attain the same spacer length as T_{20}, and T_{11}-PEG2000 was found to meet this requirement. To synthesize the conjugated spacer, we used PEG2000-DSPE with a maleimide modification to conjugate to thiol-modified AS1411-T_{11} (Figure 5A). The AS1411-T_{11}-PEG2000 conjugate was prepared by thiol-maleimide coupling at room temperature, followed by gel purification. The successful coupling of DNA–lipid conjugates was confirmed by MALDI-MS and SDS-PAGE (Figure S5). DNA–lipid conjugates were then introduced to liposomes (Apt-T_{11}-PEG2000-PEG-Lip-Dox or Ctrl-T_{11}-PEG2000-PEG-Lip-Dox) by incubating the conjugates together with other lipids during the mixing process. The PEGylated liposome modified with Apt-T_{11}-PEG2000 had a hydrodynamic size of -170 ± 28 nm and a surface zeta-potential of -15.3 ± 0.6 mV, comparable to the Apt-T_{20}-modified liposome (Figure S6).

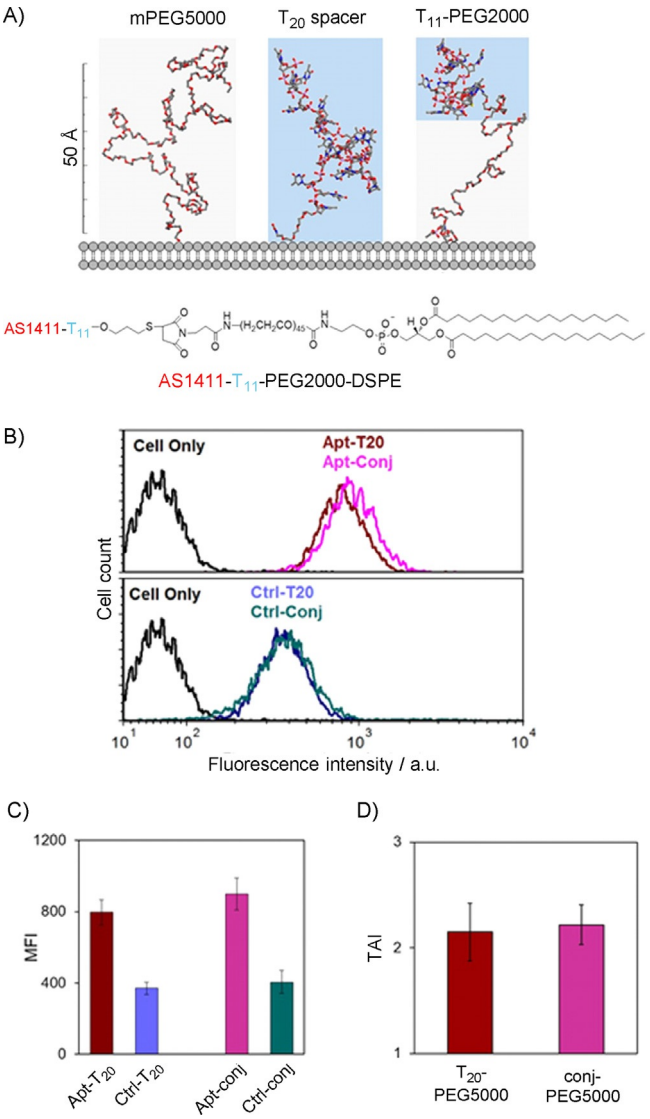

Figure 5. A) Molecular dynamics simulation of mPEG5000, T_{20}, and T_{11}-PEG2000 conjugate. The length of mPEG5000 was estimated to be ~58 Å, with T_{20} length of ~56 Å, and T_{11}-PEG2000 conjugate length of ~60 Å. B) Flow cytometry analysis of MDA-MB-231 cells treated with Apt- or Ctrl-linked T_{20}-Lip-Dox and T_{11}-PEG2000-Lip-Dox (Conj-Lip-Dox) samples. MDA-MB-231 cells (200 000 cells per well) were plated in 12-well plates. The cells were treated with liposomal Dox samples (equivalent to 20 μM Dox) at 37 °C for 2 h. C) Geometric MFI of MDA-MB-231 cells treated with liposomal Dox. D) TAI of liposomal Dox. Error bars represent the standard deviation of three experiments.

By using T_{11}-PEG2000 conjugate as the spacer, the NCL recognition motif was appended to the liposomal surface by a spacer of similar length as T_{20}, whereas the chemical composition and electrostatic charge varied. The targeting abilities of Apt-T_{11}-PEG2000-PEG-Lip-Dox and Ctrl-T_{11}-PEG2000-PEG-Lip-

Dox were analyzed by flow cytometry under the same conditions as in Figure 4. As shown in Figure 5, the MFI of MDA-MB-231 cells treated with Apt-T_{11}-PEG2000-PEG-Lip-Dox sample was significantly higher than those treated with Ctrl-T_{11}-PEG2000-PEG-Lip-Dox, suggesting the new conjugated spacer could also maintain AS1411 targeting ability. On the other hand, MDA-MB-231 cells treated with both Apt-T_{11}-PEG2000-PEG-Lip-Dox and Apt-T_{20}-PEG-Lip-Dox exhibited similar MFI and TAI values, indicating similar cell internalization properties (Figure 5D). These results suggested that the type of spacers used had a minimal effect on targeting, and that targeting could be achieved as long as the spacer could expose the recognition motif of the aptamer from PEG backfilling on the surface of liposomes.

In conclusion, we systematically investigated the interactions between the AS1411 DNA aptamer and PEG protecting groups on the surface of liposomal Dox and their effects on the cellular uptake ability and cytotoxicity of MDA-MB-231 cells. We demonstrated that the AS1411 aptamer on the liposomal surface should be fully exposed by having a spacer of appropriate length to overcome the shielding from surrounding PEG5000 molecules in order to achieve the best targeting effect. We also showed that the physical spacer length is a critical factor in determining the targeting ability of the system, regardless of the composition of the spacer, such as T_{20} or T_{11}-PEG2000. Although PEG, as a backfilling molecule, is known to help reduce non-specific serum protein absorption, it can also interact with biorecognition molecules such as the aptamer on the liposomal surface. The detailed investigation of the interaction between PEG and aptamers reported here helps further our understanding of the surface chemistry at the nano-bio-interface of this clinically used liposomal Dox system and offer important guidelines for the design of targeted drug delivery systems with better performance.

Acknowledgements

This work was supported by a seed grant from the Beckman Institute of Advanced Science and Technology and the Interdisciplinary Innovation Initiative Program at the University of Illinois at Urbana–Champaign. H.X. is a Beckman Institute Fellow at the University of Illinois at Urbana–Champaign.

Keywords: DNA aptamers · drug delivery · liposomes · PEG modification

[1] a) B. D. Chithrani, A. A. Ghazani, W. C. W. Chan, *Nano Lett.* **2006**, *6*, 662–668; b) M. E. Davis, Z. Chen, D. M. Shin, *Nat. Rev. Drug Discovery* **2008**, *7*, 771–782; c) M. Lundqvist, J. Stigler, G. Elia, I. Lynch, T. Cedervall, K. A. Dawson, *Proc. Natl. Acad. Sci. USA* **2008**, *105*, 14265–14270; d) S. L. Zhang, J. Li, G. Lykotrafitis, G. Bao, S. Suresh, *Adv. Mater.* **2009**, *21*, 419; e) E. A. Sykes, J. Chen, G. Zheng, W. C. W. Chan, *ACS Nano* **2014**, *8*, 5696–5706; f) C. D. Walkey, J. B. Olsen, H. B. Guo, A. Emili, W. C. W. Chan, *J. Am. Chem. Soc.* **2012**, *134*, 2139–2147.

[2] a) Q. Dai, C. Walkey, W. C. W. Chan, *Angew. Chem. Int. Ed.* **2014**, *53*, 5093–5096; *Angew. Chem.* **2014**, *126*, 5193–5196; b) Q. L. Liu, C. Jin, Y. Y. Wang, X. H. Fang, X. B. Zhang, Z. Chen, W. H. Tan, *NPG Asia Mater.* **2014**, *6*, e95; c) D. F. Moyano, K. Saha, G. Prakash, B. Yan, H. Kong, M. Yazdani, V. M. Rotello, *ACS Nano* **2014**, *8*, 6748–6755; d) P. C. Patel, D. A. Giljohann, W. L. Daniel, D. Zheng, A. E. Prigodich, C. A. Mirkin, *Bioconjugate Chem.* **2010**, *21*, 2250–2256; e) A. Salvati, A. S. Pitek, M. P. Monopoli, K. Prapainop, F. B. Bombelli, D. R. Hristov, P. M. Kelly, C. Aberg, E. Mahon, K. A. Dawson, *Nat. Nanotechnol.* **2013**, *8*, 137–143.

[3] a) J. D. Hood, M. Bednarski, R. Frausto, S. Guccione, R. A. Reisfeld, R. Xiang, D. A. Cheresh, *Science* **2002**, *296*, 2404–2407; b) D. Schrama, R. A. Reisfeld, J. C. Becker, *Nat. Rev. Drug Discovery* **2006**, *5*, 147–159; c) D. Simberg, T. Duza, J. H. Park, M. Essler, J. Pilch, L. L. Zhang, A. M. Derfus, M. Yang, R. M. Hoffman, S. Bhatia, M. J. Sailor, E. Ruoslahti, *Proc. Natl. Acad. Sci. USA* **2007**, *104*, 932–936; d) H. Xing, K. Hwang, J. Li, S. F. Torabi, Y. Lu, *Curr. Opin. Chem. Eng.* **2014**, *4*, 79–87; e) Y. M. Yang, F. Liu, X. G. Liu, B. G. Xing, *Nanoscale* **2013**, *5*, 231–238; f) J. M. Zhang, P. L. Yang, N. S. Gray, *Nat. Rev. Cancer* **2009**, *9*, 28–39.

[4] a) C. Tuerk, L. Gold, *J Science* **1990**, *249*, 505–510; b) A. D. Ellington, J. W. Szostak, *Nature* **1990**, *346*, 818-822; c) L. C. Bock, L. C. Griffin, J. A. Latham, E. H. Vermaas, J. J. Toole, *Nature* **1992**, *355*, 564–566.

[5] a) Z. H. Cao, R. Tong, A. Mishra, W. C. Xu, G. C. L. Wong, J. J. Cheng, Y. Lu, *Angew. Chem. Int. Ed.* **2009**, *48*, 6494–6498; *Angew. Chem.* **2009**, *121*, 6616–6620; b) O. C. Farokhzad, J. J. Cheng, B. A. Teply, I. Sherifi, S. Jon, P. W. Kantoff, J. P. Richie, R. Langer, *Proc. Natl. Acad. Sci. USA* **2006**, *103*, 6315–6320; c) J. W. Liu, Z. H. Cao, Y. Lu, *Chem. Rev.* **2009**, *109*, 1948–1998; d) S. S. Oh, K. Plakos, X. H. Lou, Y. Xiao, H. T. Soh, *Proc. Natl. Acad. Sci. USA* **2010**, *107*, 14053–14058; e) D. Shangguan, Y. Li, Z. W. Tang, Z. H. C. Cao, H. W. Chen, P. Mallikaratchy, K. Sefah, C. Y. J. Yang, W. H. Tan, *Proc. Natl. Acad. Sci. USA* **2006**, *103*, 11838–11843.

[6] a) N. L. Rosi, C. A. Mirkin, *Chem. Rev.* **2005**, *105*, 1547–1562; b) Z. Y. Xiao, O. C. Farokhzad, *ACS Nano* **2012**, *6*, 3670–3676; c) H. Xing, L. Tang, X. J. Yang, K. Hwang, W. D. Wang, Q. Yin, N. Y. Wong, L. W. Dobrucki, N. Yasui, J. A. Katzenellenbogen, W. G. Helferich, J. J. Cheng, Y. Lu, *J. Mater. Chem. B* **2013**, *1*, 5288–5297.

[7] a) T. Cedervall, I. Lynch, S. Lindman, T. Berggard, E. Thulin, H. Nilsson, K. A. Dawson, S. Linse, *Proc. Natl. Acad. Sci. USA* **2007**, *104*, 2050–2055; b) S. M. Moghimi, A. C. Hunter, J. C. Murray, *Pharmacol. Rev.* **2001**, *53*, 283–318; c) A. E. Nel, L. Madler, D. Velegol, T. Xia, E. M. V. Hoek, P. Somasundaran, F. Klaessig, V. Castranova, M. Thompson, *Nat. Mater.* **2009**, *8*, 543–557; d) C. D. Walkey, W. C. W. Chan, *Chem. Soc. Rev.* **2012**, *41*, 2780–2799.

[8] a) C. C. Fleischer, C. K. Payne, *Acc. Chem. Res.* **2014**, *47*, 2651–2659; b) S. Tenzer, D. Docter, J. Kuharev, A. Musyanovych, V. Fetz, R. Hecht, F. Schlenk, D. Fischer, K. Kiouptsi, C. Reinhardt, K. Landfester, H. Schild, M. Maskos, S. K. Knauer, R. H. Stauber, *Nat. Nanotechnol.* **2013**, *8*, 772-U1000.

[9] a) M. P. Monopoli, C. Aberg, A. Salvati, K. A. Dawson, *Nat. Nanotechnol.* **2012**, *7*, 779–786; b) M. A. Dobrovolskaia, D. R. Germolec, J. L. Weaver, *Nat. Nanotechnol.* **2009**, *4*, 411–414.

[10] a) R. Gref, M. Luck, P. Quellec, M. Marchand, E. Dellacherie, S. Harnisch, T. Blunk, R. H. Muller, *Colloids Surf. B* **2000**, *18*, 301–313; b) K. Knop, R. Hoogenboom, D. Fischer, U. S. Schubert, *Angew. Chem. Int. Ed.* **2010**, *49*, 6288–6308; *Angew. Chem.* **2010**, *122*, 6430–6452.

[11] a) J. F. Stefanick, J. D. Ashley, T. Kiziltepe, B. Bilgicer, *ACS Nano* **2013**, *7*, 2935–2947; b) P. E. Saw, J. Park, E. Lee, S. Ahn, J. Lee, H. Kim, J. Kim, M. Choi, O. C. Farokhzad, S. Jon, *Theranostics* **2015**, *5*, 746–754.

[12] a) Y. Kaneda, *Adv. Drug Delivery Rev.* **2000**, *43*, 197–205; b) J. Schäfer, S. Höbel, U. Bakowsky, A. Aigner, *Biomaterials* **2010**, *31*, 6892–6900.

[13] M. E. R. O'Brien, N. Wigler, M. Inbar, R. Rosso, E. Grischke, A. Santoro, R. Catane, D. G. Kieback, P. Tomczak, S. P. Ackland, F. Orlandi, L. Mellars, L. Alland, C. Tendler, *Ann. Oncol.* **2004**, *15*, 440–449.

[14] Y. Barenholz, *J. Controlled Release* **2012**, *160*, 117–134.

[15] J. W. Park, K. L. Hong, D. B. Kirpotin, G. Colbern, R. Shalaby, J. Baselga, Y. Shao, U. B. Nielsen, J. D. Marks, D. Moore, D. Papahadjopoulos, C. C. Benz, *Clin. Cancer Res.* **2002**, *8*, 1172–1181.

[16] S. A. Abraham, D. N. Waterhouse, L. D. Mayer, P. R. Cullis, T. D. Madden, M. B. Bally, *Methods Enzymol.* **2005**, *391*, 71–97.

[17] a) D. P. Wernette, C. Mead, P. W. Bohn, Y. Lu, *Langmuir* **2007**, *23*, 9513–9521; b) S. Balamurugan, A. Obubuafo, R. L. McCarley, S. A. Soper, D. A. Spivak, *Anal. Chem.* **2008**, *80*, 9630–9634; c) T. Hianik, I. Grman, I. Karpisova, *Chem. Commun.* **2009**, 6303–6305.

[18] a) X. G. Li, D. J. Hirsh, D. Cabral-Lilly, A. Zirkel, S. M. Gruner, A. S. Janoff, W. R. Perkins, *Biochim. Biophys. Acta Biomembr.* **1998**, *1415*, 23–40; b) A.

Fritze, F. Hens, A. Kimpfler, R. Schubert, R. Peschka-Suss, *Biochim. Biophys. Acta Biomembr.* **2006**, *1758*, 1633 – 1640.
[19] N. Dave, J. W. Liu, *Adv. Mater.* **2011**, *23*, 3182.
[20] a) J. H. Jeong, S. W. Kim, T. G. Park, *Bioconjugate Chem.* **2003**, *14*, 473 – 479; b) M. Lee, S. W. Kim, *Pharm. Res.* **2005**, *22*, 1 – 10; c) S. J. Sung, S. H. Min, K. Y. Cho, S. Lee, Y. J. Min, Y. I. Yeom, J. K. Park, *Biol. Pharm. Bull.* **2003**, *26*, 492 – 500; d) A. Malek, F. Czubayk, A. Aigner, *J. Drug Targeting* **2008**, *16*, 124 – 139.

Manuscript received: February 15, 2016
Accepted article published: April 28, 2016
Final article published: May 11, 2016